



RICE UNIVERSITY

HYPERSONIC, TWO-DIMENSIONAL POWER-LAW WINGS
OF MAXIMUM LIFT-TO-DRAG RATIO

by

WILLIAM L. WILSON

A THESIS SUBMITTED
IN PARTIAL FULFILLMENT OF THE
REQUIREMENTS FOR THE DEGREE OF
MASTER OF SCIENCE

Thesis Director's signature

Augustine

Houston, Texas

May, 1966

Abstract

HYPERSONIC, TWO-DIMENSIONAL POWER-LAW WINGS
OF MAXIMUM LIFT-TO-DRAG RATIO

by

WILLIAM L. WILSON

The problem of maximizing the lift-to-drag ratio of a slender, flat-top hypersonic wing is investigated under the assumptions that the pressure distribution is Newtonian and the skin-friction coefficient is constant. Direct methods are employed, and the analysis is confined to the class of two-dimensional wings whose chordwise contour is a power law.

First, unconstrained configurations are considered, and the combination of power law exponent and thickness ratio maximizing the lift-to-drag ratio is determined. It is found that the maximum lift-to-drag ratio is $L/D = 0.529 C_f^{-1/3}$ and corresponds to a wedge of thickness ratio $t/\lambda = 1.26 C_f^{1/3}$, where C_f is the skin-friction coefficient.

Next, constrained configurations are considered, that is, conditions are imposed on the length, the thickness, the enclosed area, and the center of pressure. For each combination of constraints, an appropriate similarity parameter is introduced, and the optimum power law exponent, thickness ratio, and the lift-to-drag ratio are determined as functions of the similarity parameter.

ACKNOWLEDGEMENTS

The author wishes to extend his appreciation to Dr. Angelo Miele for his suggestions and encouragement with regard to this work. He also wishes to thank the Langley Research Center of National Aeronautics and Space Administration under whose Grant No. NGR-44-006-034 this research was supported.

TABLE OF CONTENTS

	Page
1. Introduction-----	1
2. Fundamental Equations-----	4
3. Unconstrained Configuration-----	8
4. Given Center of Pressure-----	10
5. Given Thickness and Length-----	11
6. Given Enclosed Area and Length-----	12
7. Given Enclosed Area and Thickness-----	15
8. Discussion and Conclusions-----	17
References-----	19
List of Captions-----	21

1. INTRODUCTION

Current interest in long range vehicles capable of cruising or gliding at hypersonic speeds and maneuverable vehicles capable of reentering the earth's atmosphere from outer space missions has emphasized a definite need for configurations (bodies, wings, and wing-body combinations) with high lift-to-drag ratios. This is apparent because both the range and the maneuverability increase with the lift-to-drag ratio.

In order to determine these configurations, it is, first of all, necessary to relate the aerodynamic forces to the shapes of the bodies. At hypersonic speeds, a simple--yet quite reliable--method is the Newtonian impact theory. The basic idea of this theory is that, if the free-stream Mach number is sufficiently large, the shock wave lies so close to the body that it can be regarded to be identical with the body surface. Consequently, the pressure coefficient is determined with the assumption that the particles crossing the shock wave conserve the tangential component of the momentum but lose the normal component. With this theory, the aerodynamic characteristics were determined for particular shapes (Refs. 1 through 6), and it was concluded that, in general, the theory agrees with the experimental results quite well for sharp-nosed cones and convex configurations.

With the above assumptions and the further assumption that the skin-friction coefficient is constant, Professor Miele made an intensive research on slender, flat-top, affine wings at hypersonic speeds. In Ref. 7, analytical expressions were derived relating the drag, the lift, and the lift-to-drag ratio to the geometry

of the configuration, that is, the chordwise and spanwise contours of the affine wing. In Ref. 8, two complementary variational problems were formulated, that of optimizing the chordwise contour and that of optimizing the spanwise contour and the chord distribution, the criterion of optimization being the lift-to-drag ratio. The existence of similar solutions was investigated, and it was concluded that (1) the optimum chordwise contour of a wing of arbitrary spanwise contour and chord distribution can be determined from the known optimum chordwise contour of a wing of constant trailing edge thickness and constant chord and (2) the optimum spanwise contour and chord distribution of a wing of arbitrary chordwise contour can be determined from the known optimum spanwise contour and chord distribution of a wing of linear chordwise thickness distribution.

Because of Ref. 8, the general problem of finding the optimum configuration is reduced to that of determining the extremal properties of these reference wings. Here, a two-dimensional wing is considered, and its longitudinal contour is determined so as to yield the maximum lift-to-drag ratio, either without constraints or with constraints imposed on the length, the thickness, the enclosed area, and the position of the center of pressure. Direct methods are employed, and the analysis is confined to the class of power law contours.

The hypotheses employed are as follows: (a) the wing is two-dimensional; (b) the upper surface is flat; (c) the free-stream velocity is parallel to the plane of the flat top and is perpendicular to the base plane; (d) the pressure coefficient is twice the cosine squared of the angle formed by the free-stream velocity and

the normal to each surface element; (e) the skin-friction coefficient is constant; (f) the contribution of the tangential forces to the lift is negligible with respect to the contribution of the normal forces; (g) the wing is slender in the chordwise sense; and (h) the chordwise contour is represented by a power law.

2. FUNDAMENTAL EQUATIONS

Consider a Cartesian coordinate system Oxz (Fig. 1): the origin O is the apex of the wing; the x -axis is identical with the free-stream direction, positive leeward; and the z -axis is perpendicular to the x -axis, positive downward.

If the hypotheses (a) through (f) are invoked and if the lower surface of the wing is represented by the relationship

$$z = z(x) \quad (1)$$

the aerodynamic quantities (drag per unit span D , lift per unit span L , and pitching moment per unit span M) and the enclosed area A can be written as (Ref. 7 and 8)

$$\begin{aligned} D/q &= 2 \int_0^{\ell} \left[\dot{z}^3 / (1 + \dot{z}^2) + C_f \right] dx \\ L/q &= 2 \int_0^{\ell} \left[\dot{z}^2 / (1 + \dot{z}^2) \right] dx \\ M/q &= 2 \int_0^{\ell} \left[\dot{z}^2 (z\dot{z} + x) / (1 + \dot{z}^2) \right] dx \\ A &= \int_0^{\ell} z dx \end{aligned} \quad (2)$$

where q is the free-stream dynamic pressure, ℓ the chord, and \dot{z} the derivative dz/dx .

Next, we invoke hypothesis (g) and observe that Eqs. (2) reduce to

$$\begin{aligned}
 D/q &= 2 \int_0^{\ell} (\dot{z}^3 + C_f) dx \\
 L/q &= 2 \int_0^{\ell} \dot{z}^2 dx \\
 M/q &= 2 \int_0^{\ell} x \dot{z}^2 dx \\
 A &= \int_0^{\ell} z dx
 \end{aligned} \tag{3}$$

In accordance with hypothesis (h), we specialize the chordwise contour (1) to the power law

$$z/t = (x/\ell)^n \tag{4}$$

where n is an undetermined exponent and t is the base thickness. Consequently, Eqs. (3) become

$$\begin{aligned}
 D/q &= \left[(t^3/\ell^2) f_1 + 2C_f \ell \right] \\
 L/q &= (t^2/\ell) f_2 \\
 M/q &= t^2 f_3 \\
 A &= \ell t f_4
 \end{aligned} \tag{5}$$

in which the functions

$$\begin{aligned}
 f_1(n) &= 2n^3 / (3n - 2) \\
 f_2(n) &= 2n^2 / (2n - 1) \\
 f_3(n) &= n \\
 f_4(n) &= 1 / (n + 1)
 \end{aligned}
 \tag{6}$$

depend on the power law exponent only, and are valid for $n > 2/3$.

Certain derived quantities can be obtained from Eqs. (5). Thus, the dimensionless distance of the center of pressure from the apex $\xi_0 = x_0 / \ell = M / L\ell$ is given by

$$\xi_0 = f_3 / f_2
 \tag{7}$$

and the lift-to-drag ratio by

$$L/D = \frac{(t^2 / \ell) f_2}{(t^3 / \ell^2) f_1 + 2\ell C_f}
 \tag{8}$$

For convenience, Eq. (8) can be rewritten as

$$E = \frac{\tau^2 f_2}{\tau^3 f_1 + 2}
 \tag{9}$$

providing the lift-to-drag ratio parameter E and the thickness ratio parameter τ are defined as

$$E = (L/D) C_f^{1/3} \quad , \quad \tau = (t/l) C_f^{-1/3} \quad (10)$$

3. UNCONSTRAINED CONFIGURATION

The first step in the analysis is to determine the maximum lift-to-drag ratio of a configuration which is unconstrained geometrically and aerodynamically. According to Eq. (9), the lift-to-drag ratio parameter depends on both the thickness ratio parameter and the power law exponent, that is, it has the form $E = E(\tau, n)$. Therefore, the optimum values of τ and n are determined by the simultaneous relationships

$$E_{\tau} = 0 \quad , \quad E_n = 0 \quad (11)$$

in which the subscripts denote partial derivatives. These relationships can be written explicitly as

$$\tau^3 f_1 - 4 = 0 \quad (12)$$

$$\dot{f}_2(\tau^3 f_1 + 2) - \tau^3 \dot{f}_1 f_2 = 0$$

with the dot sign denoting a total derivative with respect to n . From Eq. (12-1), it appears that the optimum thickness ratio parameter is such that the skin-friction drag is one-third of the total drag. Furthermore, upon eliminating the thickness ratio parameter from Eqs. (12), we obtain the relationship

$$2g_1 - 3g_2 = 0 \quad (13)$$

where

$$g_1 = \dot{f}_1/f_1 \quad , \quad g_2 = \dot{f}_2/f_2 \quad (14)$$

On account of the definitions (6-1) and (6-2), we see that Eq. (13) is solved by

$$n = 1 \quad (15)$$

which means that the optimum chordwise contour is a wedge. With this understanding, the thickness ratio parameter (12-1) and the lift-to-drag ratio parameter (9) become

$$\begin{aligned} \tau &= \sqrt[3]{2} \cong 1.26 \\ E &= 2/3 \sqrt[3]{2} \cong 0.529 \end{aligned} \quad (16)$$

Equation (16-2) represents the upper limit to the lift-to-drag ratio which can be obtained with a two-dimensional, flat-top configuration subjected to a flow parallel to the flat top. Should the configuration be required to satisfy a certain number of geometric and/or aerodynamic constraints, a loss in the lift-to-drag ratio would occur with respect to that predicted by Eq. (16-2).

4. GIVEN CENTER OF PRESSURE

To prescribe the nondimensional distance of the center of pressure from the apex is equivalent to prescribing the power law exponent in accordance with Eq. (7). Therefore, the lift-to-drag ratio parameter can be maximized with respect to the thickness ratio parameter only, and the relevant optimum condition is represented by Eq. (11-1) implicitly or Eq. (12-1) explicitly. Because of Eq. (12-1), the optimum thickness ratio parameter is given by

$$\tau = (4/f_1)^{1/3} \quad (17)$$

and the associated lift-to-drag ratio parameter is

$$E = (f_2/3)(2/f_1^2)^{1/3} \quad (18)$$

The parametric equations (7), (17), and (18) admit solutions of the form

$$n = P(\xi_0) \quad , \quad \tau = Q(\xi_0) \quad , \quad E = R(\xi_0) \quad (19)$$

which are plotted in Figs. 2 through 4. For $\xi_0 = 1/2$, the chordwise contour is that of a wedge, and the maximum lift-to-drag ratio parameter reaches the upper limit represented by Eq. (16-2). For any other values of ξ_0 , lower values of the lift-to-drag ratio parameter are obtained as shown in Fig. 4.

5. GIVEN THICKNESS AND LENGTH

To prescribe the thickness and the length is equivalent to prescribing the thickness ratio parameter τ in accordance with the definition (10-2). Therefore, the lift-to-drag ratio parameter (9) can be maximized with respect to the power law exponent only, and the relevant optimum condition is represented by Eq. (11-2) implicitly or Eq. (12-2) explicitly. Because of Eq. (12-2), the optimum power law exponent satisfies the relationship

$$\tau = \left(\frac{2}{g_1 - g_2} \right)^{1/3} \left(\frac{f_1}{g_2} \right)^{-1/3} \quad (20)$$

The associated lift-to-drag ratio parameter is given by

$$E = \left(\frac{2}{g_1 - g_2} \right)^{-1/3} \left(\frac{f_1}{g_2} \right)^{-2/3} \left(\frac{f_2}{g_1} \right) \quad (21)$$

The parametric equations (20) and (21) admit solutions of the form^(*)

$$n = P(\tau) \quad , \quad E = R(\tau) \quad (22)$$

which are plotted in Figs. 5 and 6. If the thickness-length parameter is smaller than 0.825, the configuration is concave. If the thickness-length parameter is larger than 0.825, the configuration is a wedge which, for $\tau = 1.26$, has the lift-to-drag ratio parameter $E = 0.529$.

(*) The functions (22) are triple-valued for $\tau \leq 0.830$ and single-valued for $\tau > 0.830$. In the former case, there is one relative minimum solution and two relative maximum solutions. Among the latter, one must determine the absolute maximum solution by direct comparison of the lift-to-drag ratio parameter. This maximum solution is plotted in Figs. 5 and 6.

6. GIVEN ENCLOSED AREA AND LENGTH

If the enclosed area and the length are given, it is convenient to rewrite Eq. (5-4) in the form

$$K_1 = \tau f_4 \quad (23)$$

where

$$K_1 = (A/\ell^2) C_f^{-1/3} \quad (24)$$

is the area-thickness parameter, a known quantity. The lift-to-drag ratio parameter (9) is to be maximized with respect to the combinations of τ and n which ensure the constancy of the right-hand side of Eq. (23). In accordance with Lagrange multiplier theory, we introduce an undetermined constant λ and define the fundamental function

$$F = E + \lambda \tau f_4 \quad (25)$$

Then, the optimum conditions are

$$F_\tau = 0 \quad , \quad F_n = 0 \quad (26)$$

which are equivalent to

$$E_\tau + \lambda f_4 = 0 \quad , \quad E_n + \lambda \tau f_4 = 0 \quad (27)$$

and, upon elimination of the Lagrange multiplier, imply that

$$\tau g_4 E_\tau - E_n = 0 \quad (28)$$

where

$$g_4 = \dot{f}_4 / f_4 \quad (29)$$

In the light of Eq. (9), Eq. (28) can be rewritten as

$$\tau = \left(\frac{2}{g_1 - g_2 - g_4} \right)^{1/3} \left(\frac{f_1}{g_2 - 2g_4} \right)^{-1/3} \quad (30)$$

The associated lift-to-drag ratio parameter and area-length parameter are given by

$$E = \left(\frac{2}{g_1 - g_2 - g_4} \right)^{-1/3} \left(\frac{f_1}{g_2 - 2g_4} \right)^{-2/3} \left(\frac{f_2}{g_1 - 3g_4} \right) \quad (31)$$

$$K_1 = \left(\frac{2}{g_1 - g_2 - g_4} \right)^{1/3} \left(\frac{f_1}{g_2 - 2g_4} \right)^{-1/3} f_4$$

The parametric equations (30) and (31) admit solutions of the form^(*)

$$n = P(K_1) \quad , \quad \tau = Q(K_1) \quad , \quad E = R(K_1)$$

^(*) The functions (32) are triple-valued for $K_1 \leq 0.165$ and single-valued for $K_1 > 0.165$. In the former case, there is one relative minimum solution and two relative maximum solutions. Among the latter, one must determine the absolute maximum solution by direct comparison of the lift-to-drag ratio parameter. This maximum solution is plotted in Figs. 7 through 9.

which are plotted in Figs. 7 through 9. When the area-length parameter has the value 0.630, the configuration is a wedge with a thickness ratio parameter $\tau = 1.26$ and a lift-to-drag ratio parameter $E = 0.529$. For larger values of the area-length parameter, the configuration is convex, and for smaller values, it is concave.

7. GIVEN ENCLOSED AREA AND THICKNESS

If the enclosed area and the thickness are given, it is convenient to rewrite Eq. (5-4) in the form

$$K_2 = f_4 / \tau \quad (33)$$

where

$$K_2 = (A/t^2) C_f^{1/3} \quad (34)$$

is the area-thickness parameter, a known quantity. The lift-to-drag ratio parameter (9) is to be maximized with respect to the combinations of τ and n which ensure the constancy of the right-hand side of Eq. (33). In accordance with Lagrange multiplier theory, we introduce an undetermined constant λ and define the fundamental function

$$F = E + \lambda f_4 / \tau \quad (35)$$

Then, the optimum conditions are

$$F_\tau = 0 \quad , \quad F_n = 0 \quad (36)$$

which are equivalent to

$$\tau^2 E_\tau - \lambda f_4 = 0 \quad , \quad \tau E_n + \lambda f_4 = 0 \quad (37)$$

and, upon elimination of the Lagrange multiplier, imply that

$$\tau g_4 E_\tau + E_n = 0 \quad (38)$$

In the light of Eq. (9), Eq. (38) can be rewritten as

$$\tau = \left(\frac{2}{g_1 - g_2 + g_4} \right)^{1/3} \left(\frac{f_1}{g_2 + 2g_4} \right)^{-1/3} \quad (39)$$

The associated lift-to-drag ratio parameter and area-thickness parameter are given by

$$E = \left(\frac{2}{g_1 - g_2 + g_4} \right)^{-1/3} \left(\frac{f_1}{g_2 + 2g_4} \right)^{-2/3} \left(\frac{f_2}{g_1 + 3g_4} \right) \quad (40)$$

$$K_2 = \left(\frac{2}{g_1 - g_2 + g_4} \right)^{-1/3} \left(\frac{f_1}{g_2 + 2g_4} \right)^{1/3} f_4$$

The parametric equations (39) and (40) admit solutions of the form

$$n = P(K_2) \quad , \quad \tau = Q(K_2) \quad , \quad E = R(K_2) \quad (41)$$

which are plotted in Figs. 10 through 12. When the area-thickness parameter has the values 0.397, the configuration is a wedge, with a thickness ratio parameter $\tau = 1.26$ and a lift-to-drag ratio parameter $E = 0.529$. For larger values of the area-thickness parameter, the configuration is convex, and for smaller values, it is concave.

8. DISCUSSION AND CONCLUSIONS

In the previous sections, the problem of maximizing the lift-to-drag ratio of a slender, flat-top, hypersonic wing is investigated under the assumptions that the pressure distribution is Newtonian and the skin-friction coefficient is constant. Direct methods are employed, and the analysis is confined to the class of two-dimensional wings whose longitudinal contour is a power law.

First, unconstrained configurations are considered, and the combination of thickness ratio and power law exponent maximizing the lift-to-drag ratio is determined. For a friction coefficient $C_f = 10^{-3}$, the maximum lift-to-drag ratio is $L/D = 5.29$ and corresponds to a wedge of thickness ratio $t/\ell = 0.126$.

Next, constrained configurations are considered, that is, conditions are imposed on the length, the thickness, the enclosed area, and the position of the center of pressure. For each case, an appropriate similarity parameter is introduced, and the optimum power law exponent, thickness ratio, and lift-to-drag ratio are determined as functions of the similarity parameter. The lift-to-drag ratio of a constrained configuration is smaller than that of the optimum unconstrained configuration; however, for a particular value of the similarity parameter, equality is achieved.

While the chordwise contour is that of a wedge for an unconstrained configuration, it can be either convex or concave for constrained configurations, depending on the value of the similarity parameter. Since the Newtonian pressure law has been verified experimentally for convex configurations only, the results pertaining to concave configurations are merely indicative of qualitative trends.

To examine how closely the true optimum configurations can be approximated by power law wings, a comparison with the results obtained in Ref. 9 using the indirect method of the calculus of variations is in order. For unconstrained configurations, the solutions obtained by direct methods and those obtained by indirect methods are identical. For constrained configurations, the solutions are almost identical as long as $(t/\ell)C_f^{-1/3} \geq 1.26$ (given t and ℓ), as long as $(A/t^2)C_f^{-1/3} \leq 0.5$ (given t and A), and as long as $(A/\ell^2)C_f^{1/3} \geq 0.545$ (given ℓ and A). For other values of the similarity parameters, the differences are more significant.

Finally, it is of interest to compare the present lift-to-drag ratios with those characteristic of drag-optimized, flat-top configurations. The analysis is omitted for the sake of brevity, since it involves only a slight modification of that presented in Ref. 10. As expected, the lift-to-drag ratio of a minimum drag configuration is lower than that of a maximum lift-to-drag ratio configuration. The relative differences depend on the similarity parameter and are shown in Figs. 5 through 12.

REFERENCES

1. GRIMMINGER, G., WILLIAMS, E.P. and YOUNG, G.B.W., Lift on Inclined Bodies of Revolution in Hypersonic Flow, JAS, Vol. 17, No. 11, 1950.
2. SEAMAN, D.G. and DORE, F.J., Force and Pressure Coefficients of Elliptic Cones and Cylinders in Newtonian Flow, Convair, Report No. ZA-7-004, 1952.
3. RAINEY, R.W., Working Charts for Rapid Prediction of Force and Pressure Coefficients on Arbitrary Bodies of Revolution by Use of Newtonian Concepts, NASA, TN No. D-176, 1959.
4. FISHER, L.R., Equations and Charts for Determining the Hypersonic Stability Derivatives of Combinations of Cone Frustrums Computer by Newtonian Impact Theory, NASA, TN No. D-149, 1959.
5. MARGOLIS, K., Theoretical Evaluation of the Pressures, Forces, and Moments at Hypersonic Speeds Acting on Arbitrary Bodies of Revolution Undergoing Separate and Combined Angle-of-Attack and Pitching Motions, NASA, TN No. D-652, 1961.
6. WELLS, W.R. and ARMSTRONG, W.O., Tables of Aerodynamic Coefficients Obtained from Developed Newtonian Expressions for Complete and Partial Conic and Spheric Bodies at Combined Angles of Attack and Sideslip with Some Comparison with Hypersonic Experimental Data, NASA, TR No. R-127, 1962.

7. MIELE, A., Lift-to-Drag Ratios of Slender, Wings at Hypersonic Speeds, Rice University, Aero-Astronautics Report No. 13, 1966.
8. MIELE, A., Similarity Laws for Wings Maximizing the Lift-to-Drag Ratio at Hypersonic Speeds (in preparation).
9. HULL, D.G., Two-Dimensional Wings of Maximum Lift-to-Drag Ratio in Hypersonic Flow, Rice University, Aero-Astronautics Report No. 25, 1966.
10. SAARIS, G.R., Slender, Two-Dimensional Power Bodies Having Minimum Zero-Lift Drag in Hypersonic Flow, NASA, TR No. 76, 1963.

LIST OF CAPTIONS

- Fig. 1 Coordinate system.
- Fig. 2 Power law exponent (given center of pressure).
- Fig. 3 Optimum thickness ratio parameter (given center of pressure).
- Fig. 4 Maximum lift-to-drag ratio parameter (given center of pressure).
- Fig. 5 Optimum power law exponent (given thickness and length).
- Fig. 6 Maximum lift-to-drag ratio parameter (given thickness and length).
- Fig. 7 Optimum power law exponent (given enclosed area and length).
- Fig. 8 Optimum thickness ratio parameter (given enclosed area and length).
- Fig. 9 Maximum lift-to-drag ratio parameter (given enclosed area and length).
- Fig. 10 Optimum power law exponent (given enclosed area and thickness).
- Fig. 11 Optimum thickness ratio parameter (given enclosed area and thickness).
- Fig. 12 Maximum lift-to-drag ratio parameter (given enclosed area and thickness).

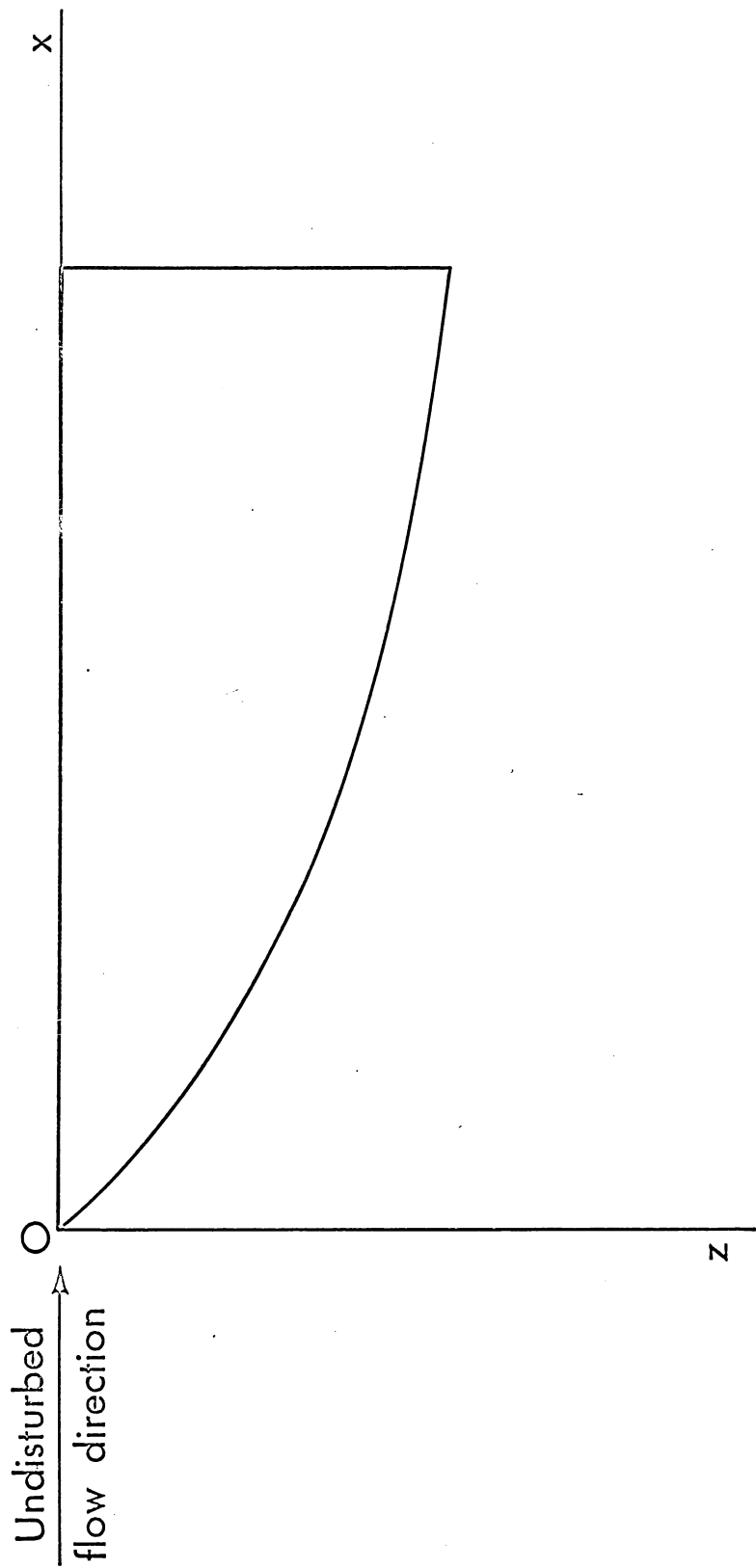


Figure 1

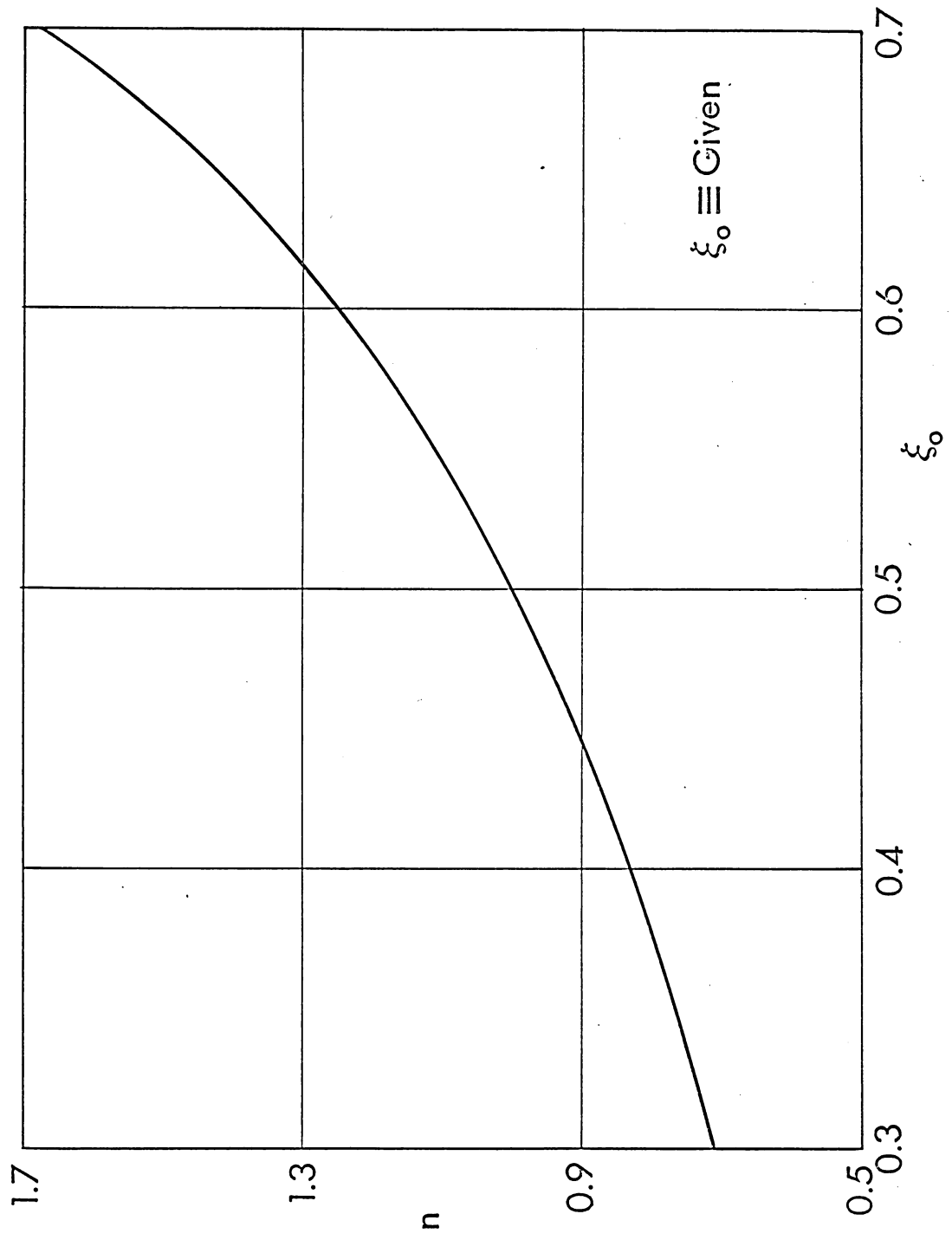


Figure 2

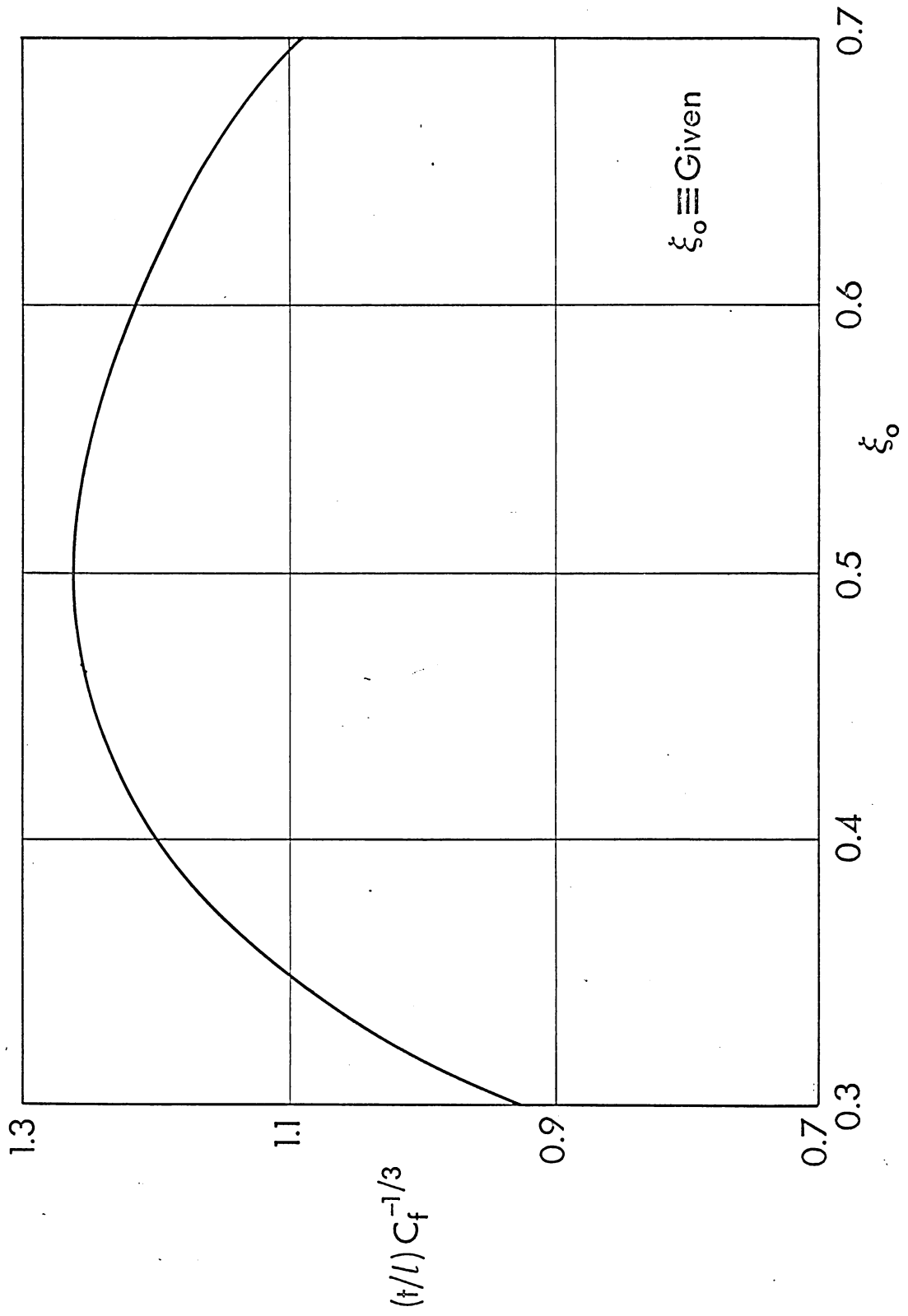


Figure 3

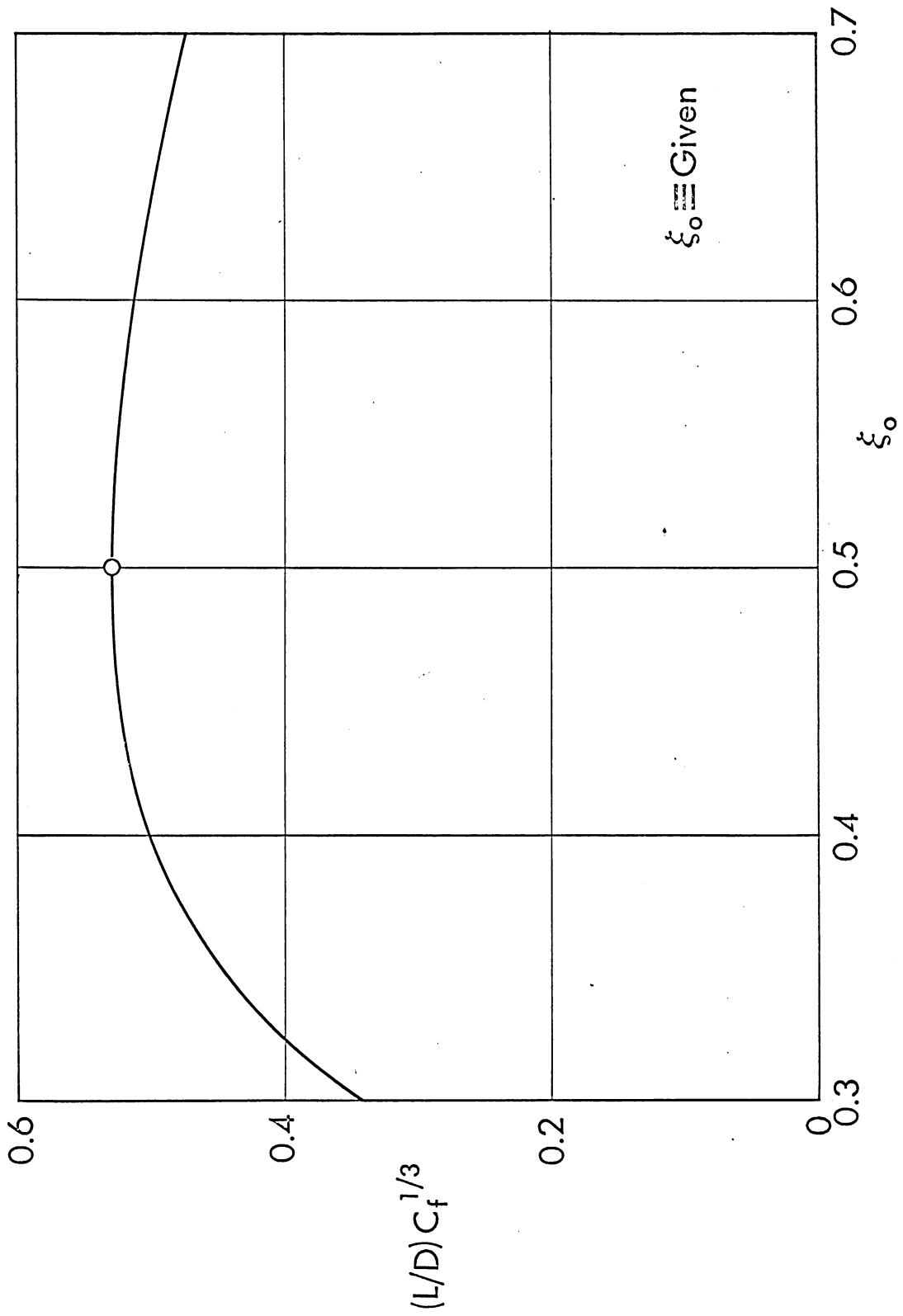


Figure 4

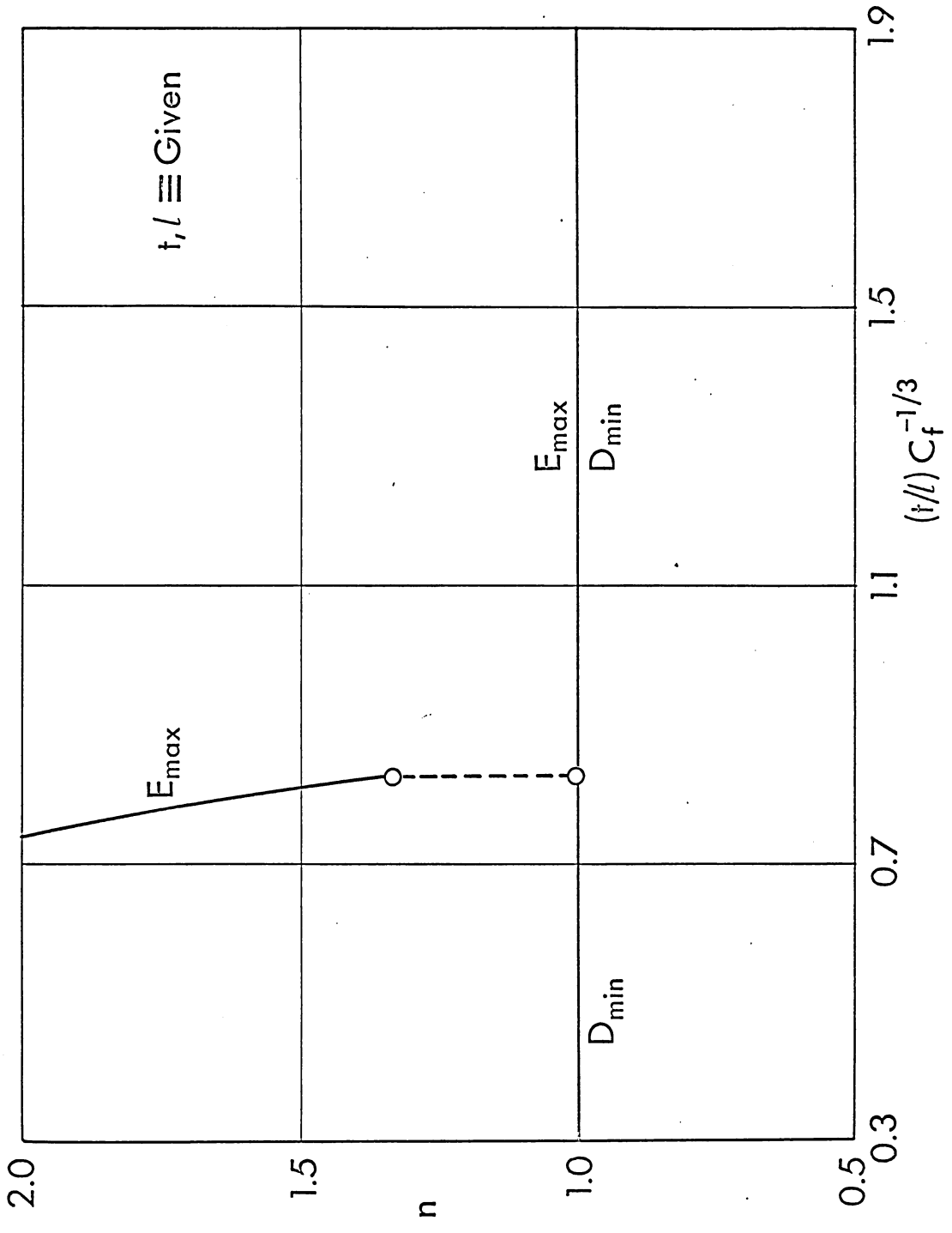


Figure 5

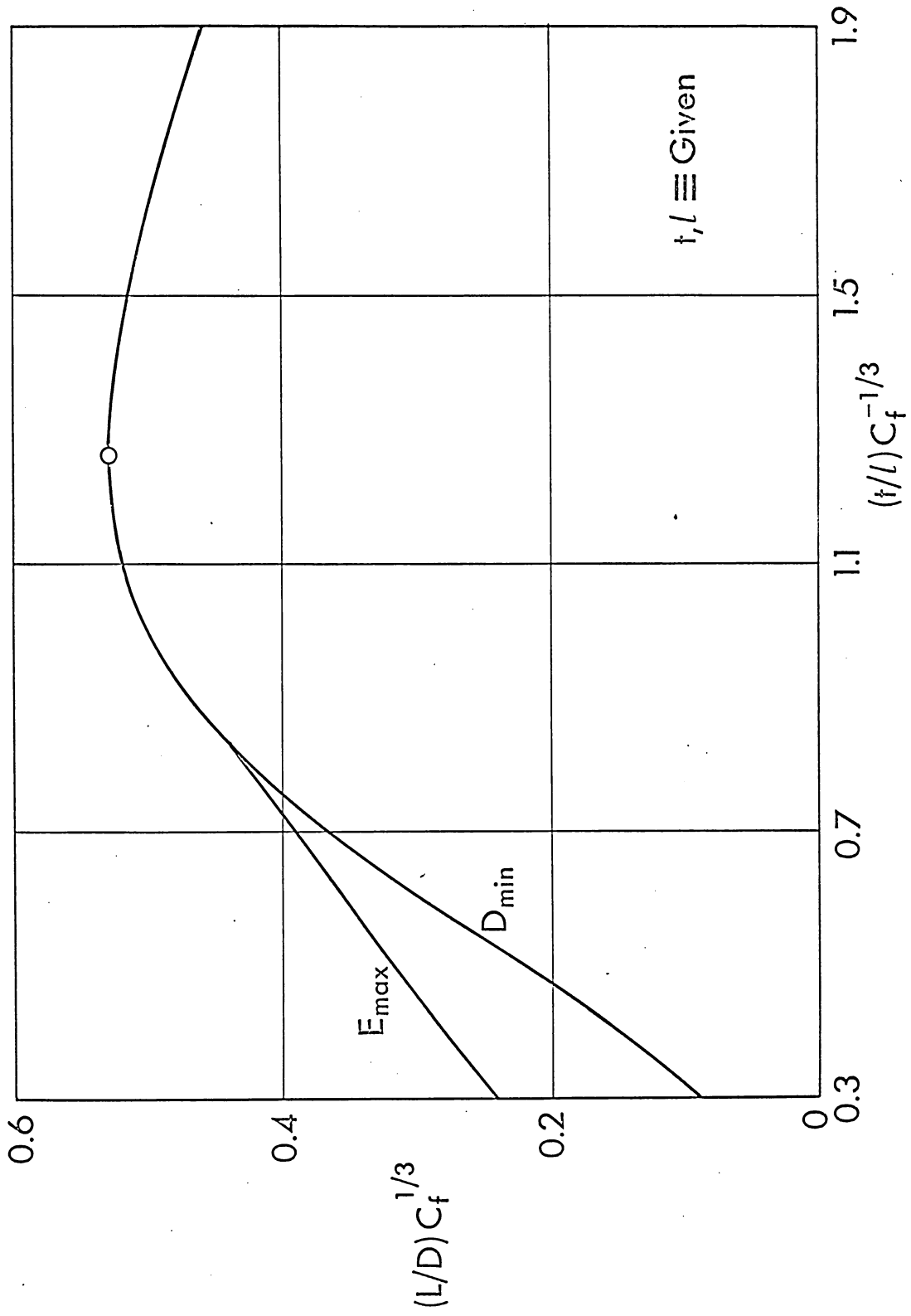


Figure 6

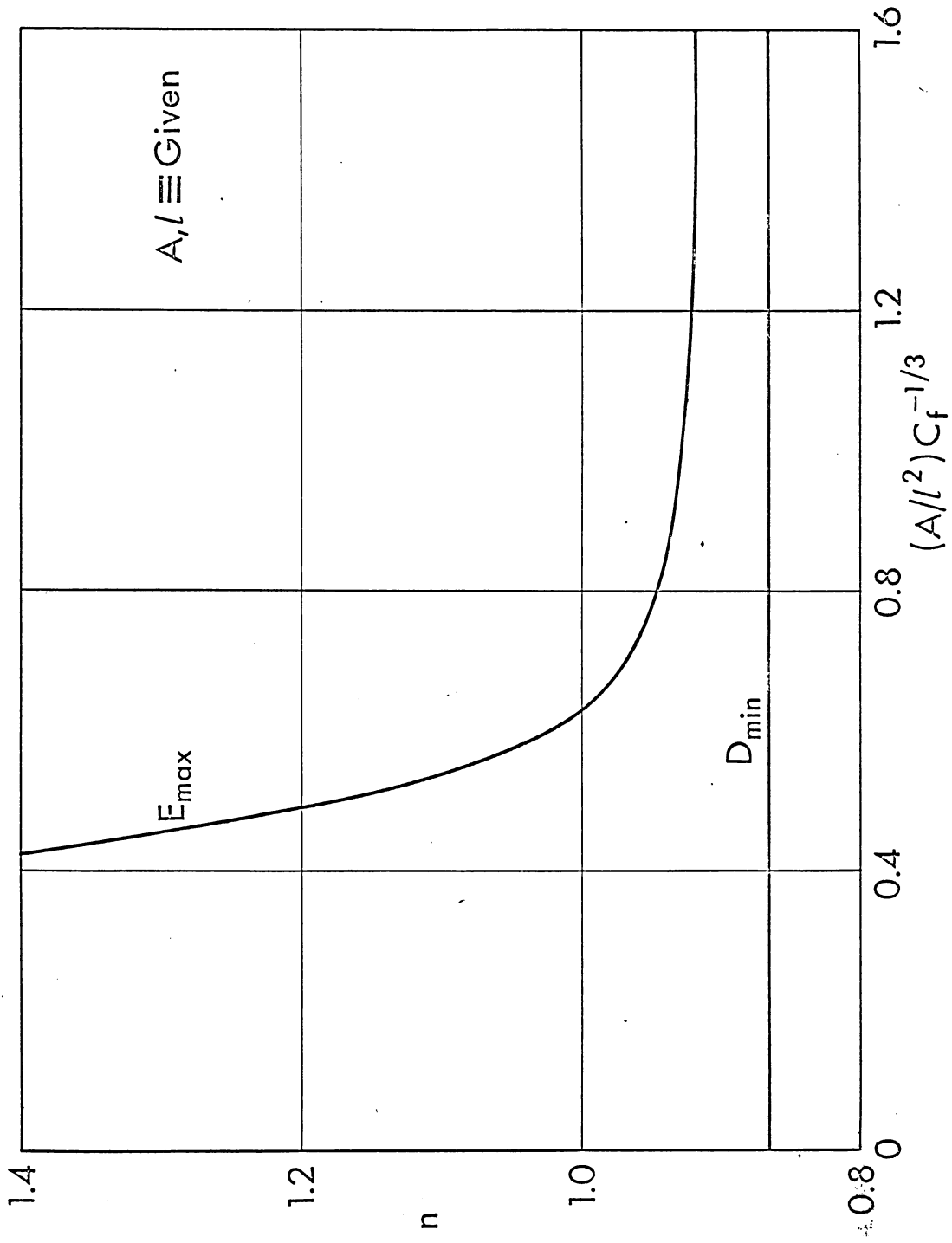


Figure 7

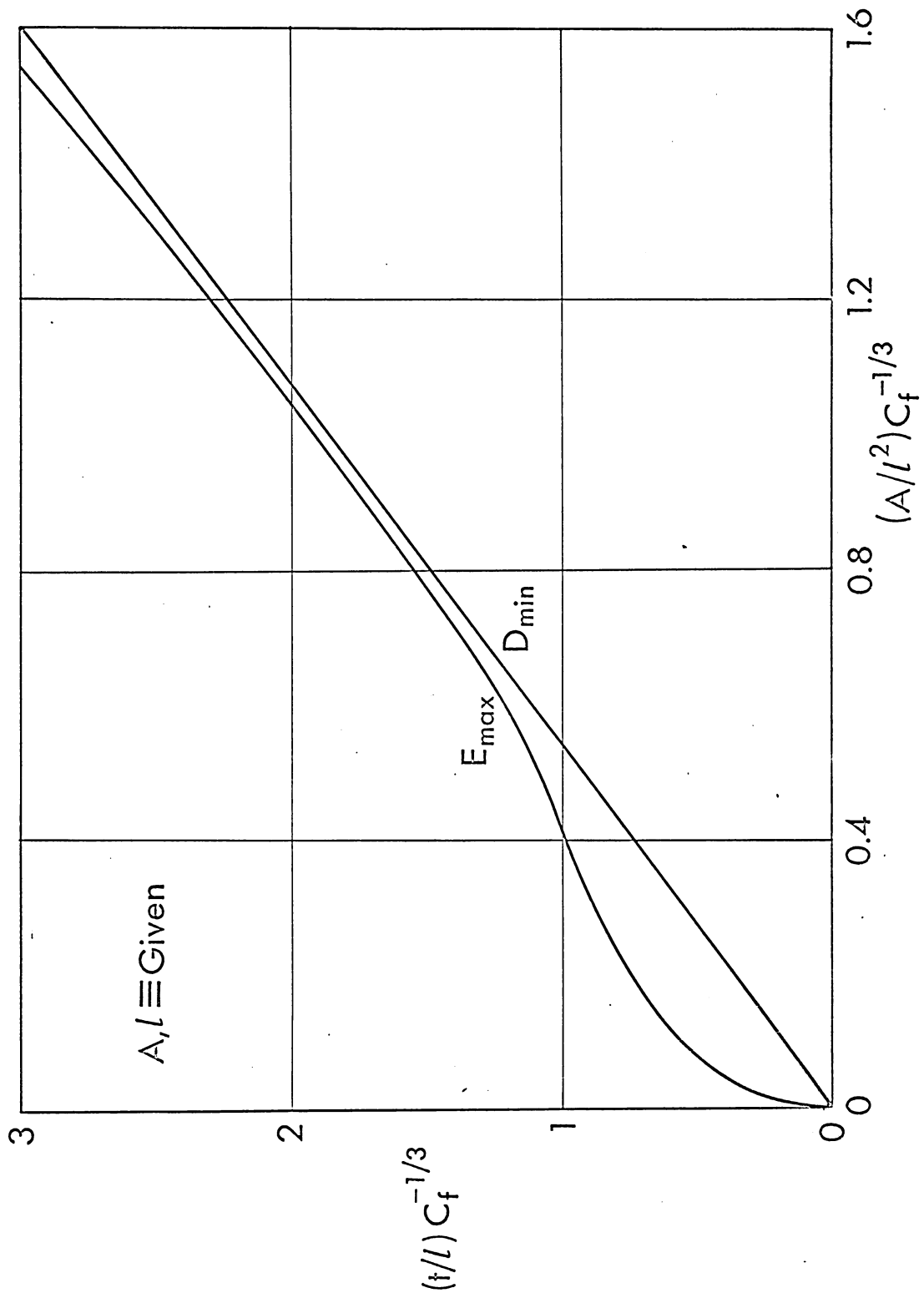


Figure 8

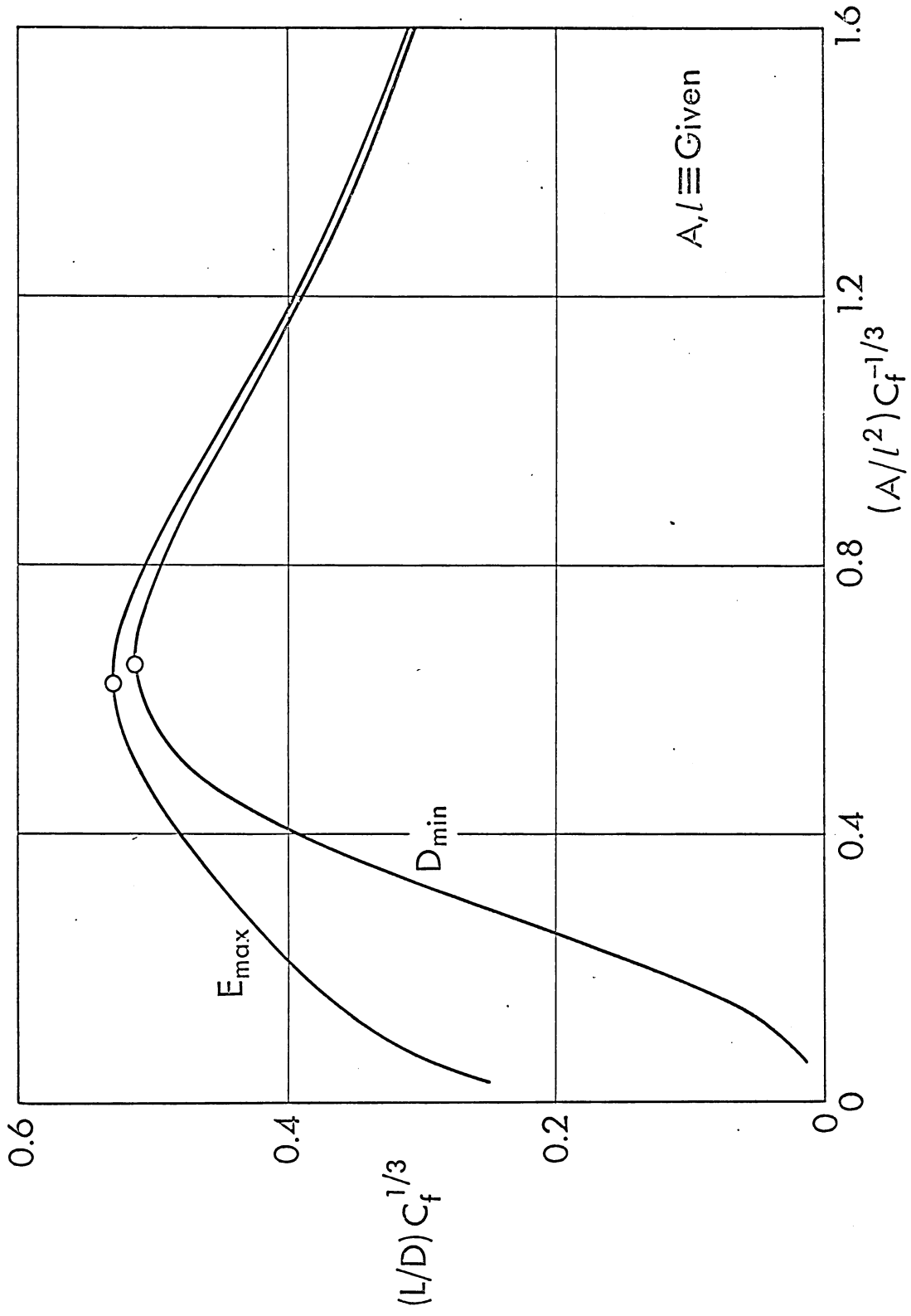


Figure 9

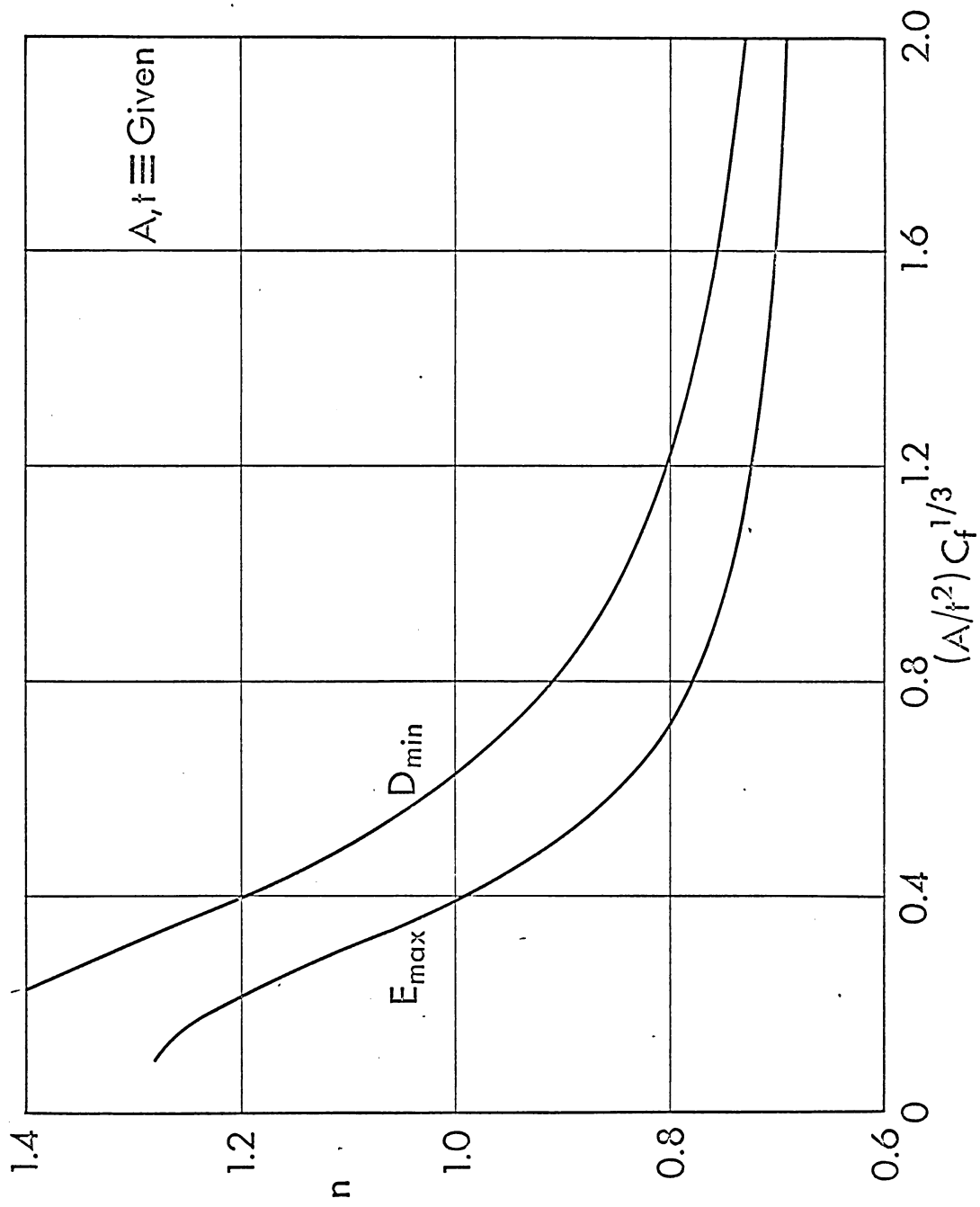


Figure 10

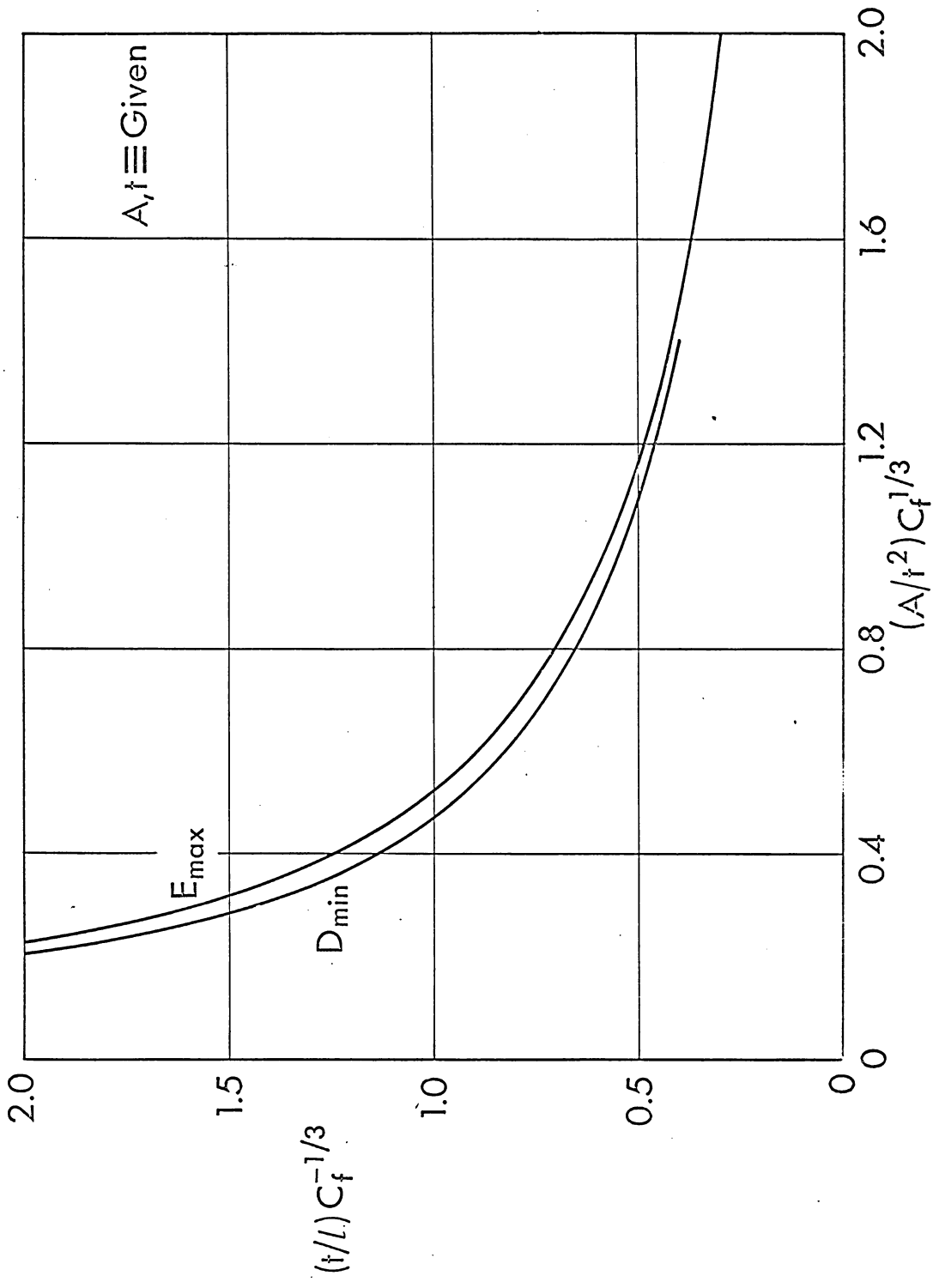


Figure 11

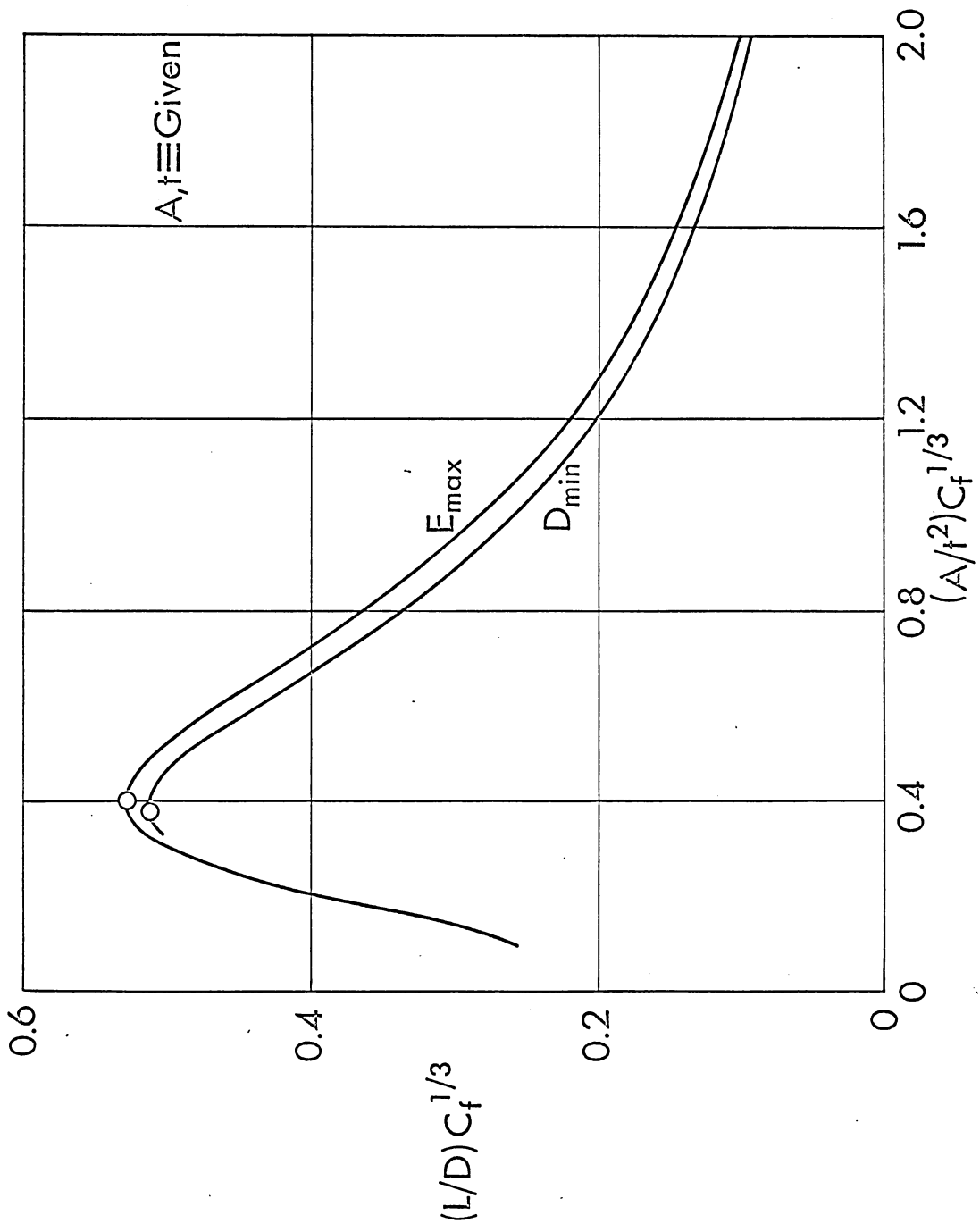


Figure 12